Thin Solid Films, *156* (1988) 127–143
PREPARATION AND CHARACTERIZATION

LONG-TIME AIR OXIDATION AND OXIDE–SUBSTRATE REACTIONS ON GaSb, GaAs AND GaP AT ROOM TEMPERATURE STUDIED BY X-RAY PHOTOELECTRON SPECTROSCOPY

YUSUKE MIZOKAWA, OSAMU KOMODA AND SUNAO MIYASE
College of Integrated Arts and Sciences, University of Osaka Prefecture, Sakai, Osaka 591 (Japan)
(Received June 26, 1987; accepted July 31, 1987)

The room temperature oxidation behaviour of GaSb, GaAs and GaP has been monitored for a period of 3 years using X-ray photoelectron spectroscopy. By comparisons of the compositions of the growing oxide and the depth profiles of the 3-year oxide, information on the oxide–substrate interfacial reactions is obtained. The growing oxide surface consists of Ga_2O_3 and Sb_2O_3 (Sb:Ga $\approx$ 1) for GaSb, a metastable Ga–O–As complex (As:Ga $\approx$ 0.5) for GaAs, and P_2O_5 and $Ga_2O_3 + GaPO_4$ (P:Ga $\approx$ 3) for GaP. The oxide–substrate reaction occurs for GaSb and GaAs, and the resulting interface shows three features: (1) increase in gallium oxide; (2) decrease in the B^V oxide; (3) deposition of elemental B^V, even at room temperature, although a very long period of time is necessary. For GaP, no such reaction occurs; instead, the reaction $16Ga + 3P_2O_5 \rightarrow 5Ga_2O_3 + 6GaP$ at the interface is predicted, where the elemental gallium has been produced by a preferential chemical etching.

1. INTRODUCTION

Native oxides on $A^{III}B^V$ compound semiconductors and the interfacial oxide–substrate chemical reactions are of considerable interest because of their close relationship to the electrical properties of metal–oxide–semiconductor devices. It is recognized that the instability of III–V metal–insulator–semiconductor (MIS) devices is related to the quality of the semiconductor–insulator interface. The chemical composition and formation of thermal and anodic oxide–(III–V) compound semiconductor interfaces have been reviewed by Wilmsen[1,2]. His papers provide very useful insight into "what is the chemical composition of the oxide–(III–V) interface" and "how and why did it get that way". As far as long-term device stability is concerned, it is very important to understand the chemistry of surface oxide formation and the reaction between oxide and substrate semiconductor during a long period at room temperature[3,4]. Such studies on a room temperature air-grown oxide (natural oxide) are also very significant since most real MIS devices contain an interfacial natural oxide layer. To date, the growth kinetics and the composition of room temperature air-grown oxides on chemically etched surfaces of $A^{III}B^V$ semiconductors have not been sufficiently investigated[5–11].

0040-6090/88/$3.50

In this paper, we report the room temperature oxidation of GaB^V compound semiconductors (GaSb, GaAs and GaP) monitored for 3 years using X-ray photoelectron spectroscopy (XPS). The grown oxide films were then depth profiled to obtain information on the interfacial oxide–substrate reactions[11,12]. Evidence is presented for the interfacial reaction between the natural oxide and GaB^V substrate even at room temperature during a prolonged time interval.

2. EXPERIMENTAL DETAILS

X-ray photoemission spectra were recorded using a DuPont electron spectroscopy for chemical analysis 650B spectrometer with Mg Kα (1253.6 eV) radiation. The ejection angle of the detected photoelectrons is surface normal. The spectrometer base pressure was in the high 10^{-8} Torr region. The samples were all (111)-oriented GaAs ($p = 9.5 \times 10^{18}\,cm^{-3}$), GaP ($p = 5.6 \times 10^{17}\,cm^{-3}$) and GaSb ($p = 1.5 \times 10^{17}\,cm^{-3}$). The substrate was etched in a solution of hydrochloric acid for 1 min and quickly rinsed in methyl alcohol. The oxidation was carried out at room temperature in desiccator for 3 years. The Ga 3d, Ga Auger $L_3M_{4,5}M_{4,5}$ (Ga LMM), Ga 2p, As 3d, P 2p, Sb $3d_{3/2}$, Sb 4d, O 1s and C 1s XPS spectra were monitored as a function of air exposure time. At least 20 measurements were carried out in that time interval for each sample. Photoelectrons with kinetic energies of about 1 keV have escape depths of about 20 Å. After 3 years had elapsed, the natural oxide films were depth profiled by 2 keV Ar^+ ion sputtering. The chemical composition was obtained after correction for preferential sputtering as described in previous papers[11,13].

3. RESULTS

3.1. Standard samples

The binding energies (BEs) (including the apparent BEs of Auger electrons) and the full widths at half-maximum (FWHMs) for Ga LMM, Ga 3d, Sb $3d_{3/2}$, As 3d, P 2p, and O 1s electrons from gallium, antimony, arsenic, phosphorus, GaSb, GaAs, GaP, Ga_2O_3, Sb_2O_3, As_2O_3, As_2O_5, P_2O_5 and $GaPO_4$ are given in Table I[13,14]. The BEs in III–V compound semiconductor surfaces were changed by the different methods of surface preparation, so the values for the cleaved (cl-), chemically etched (ch-) and sputtered (sp-) surfaces are given. All standard samples except $GaPO_4$ were obtained commercially. Since a standard sample of $GaPO_4$ was not available, the $GaPO_4$ represents a thermal oxide of GaP grown at above 1200 °C (ref. 15). All BEs except those for the sputtered samples were referred to the Au $4f_{7/2}$ level at 83.8 eV from thin gold film deposited on the sample. The gold deposition reduced the peak intensity of photoelectrons with a mean free path of about 20 Å to about one-half of its initial value. Thus the average thickness of the gold film is estimated to be about 15 Å, so the size effects[16] on the BEs may be considered negligible. The BEs for the sputtered samples were referred to the C 1s level at 285.0 eV from hydrocarbon contamination, since gold deposition on these samples changed their surface chemical structure[17]. We have also included the BE difference between Ga LMM and Ga 3d electrons, which is useful for the chemical identification of gallium

TABLE I

BINDING ENERGIES IN III–V COMPOUND SEMICONDUCTORS AND RELATED MATERIALS

Sample	*Binding energies (FWHMs)* (eV)						
	Ga LMM	*Ga 3d*	*Sb 3d 3/2*	*As 3d*	*P 2p*	*O 1s*	*ΔE (Ga LMM-Ga 3d)*
Ga	185.2 (1.5)	18.2 (1.3)					167.0
Sb			537.6 (1.4)				
As				41.6 (1.6)			
P					129.6 (1.8)		
cl-GaSb	186.7 (2.0)	18.9 (1.2)	537.4 (1.2)				167.8
ch-GaSb	186.8 (2.3)	19.0 (1.3)	537.4 (1.4)				167.8
sp-GaSb	186.0 (2.5)	18.6 (1.5)	537.2 (1.4)				167.5
cl-GaAs	187.4 (1.9)	19.2 (1.3)		41.2 (1.5)			168.2
ch-GaAs	187.1 (1.7)	19.1 (1.3)		41.1 (1.7)			168.1
sp-GaAs	186.7 (2.6)	19.0 (1.5)		41.0 (1.8)			167.8
cl-GaP	187.8 (2.2)	19.4 (1.4)			128.9 (1.6)		168.4
ch-GaP	187.6 (2.4)	19.3 (1.4)			128.9 (1.8)		168.4
sp-GaP	187.1 (3.1)	19.1 (1.9)			129.0 (2.1)		168.1
Ga_2O_3	191.6 (3.3)	20.9 (1.9)				531.8 (2.1)	170.7
Sb_2O_3			539.9 (2.0)				
As_2O_3				44.6 (1.8)		531.6 (2.0)	
As_2O_5				45.7 (2.1)		531.6 (2.2)	
P_2O_5					134.5 (2.4)	533.2 (3.5)	
$GaPO_4$	193.5 (3.9)	21.7 (1.9)			134.8 (2.1)	532.9 (2.1)	171.8

compounds even when charging and/or changes in the surface Fermi level pinning energy are present[14,17]. Other energy differences such as that between O 1s and P 2p are also used for chemical identification purposes.

As seen in Table I, the BEs of Ga LMM and Ga 3d in the GaB^V compound increase in the order GaSb < GaAs < GaP in agreement with Pauling's electronegativities X of the B^V elements ($X_{Sb} = 1.9$, $X_{As} = 2.0$, $X_P = 2.1$) and the heats of formation ΔH of GaB^V ($\Delta H_{GaSb} = -10$ kcal mol^{-1}, $\Delta H_{GaAs} = -17$ kcal mol^{-1}, $\Delta H_{GaP} = -24.4$ kcal mol^{-1}). Both the BEs and the FWHMs for the chemically etched surfaces of GaB^V compounds are in close agreement with the corresponding values for the cleaved surfaces. For quantitative analysis, the relative atomic sensitivity A_i was determined experimentally assuming that the cleaved surface of GaB^V is stoichiometric. The A_i values used for the quantitative analysis are 1, 1.5, 1, 3.4 and 1.9 for Ga 3d, As 3d, P 2p, Sb 4d and O 1s respectively. These values are in good agreement with the corresponding photoelectron cross-sections[18]. The ion sputtering of GaB^V compounds resulted in a gallium-rich surface. To obtain quantitative depth profiles of the native oxide films, the preferential sputtering coefficient $S(B^V{:}Ga)$ was determined experimentally[13]: the values are $S(As{:}Ga) \approx 1.2$, $S(P{:}Ga) \approx 1.3$ and $S(Sb{:}Ga) \approx 1.1$.

3.2. Room temperature oxidation of GaSb, GaAs and GaP

The XPS spectra from the surfaces of GaSb, GaAs and GaP were monitored during a 3 year time interval. Figure 1 shows the resulting typical spectra of Ga LMM, Sb $3d_{3/2}$, As 3d and P 2p as a function of air exposure time (several seconds, 10 min, 25 h, 554 days and 3 years from the bottom to top in each series of spectra). The chemical shifts of Ga 3d and Sb 4d are so small (about 1 eV) that Ga LMM and Sb $3d_{3/2}$ spectra were used for both the identification of the chemical state and the calculation of the ratio of the number of oxidized atoms to the number of unoxidized atoms for gallium and antimony.

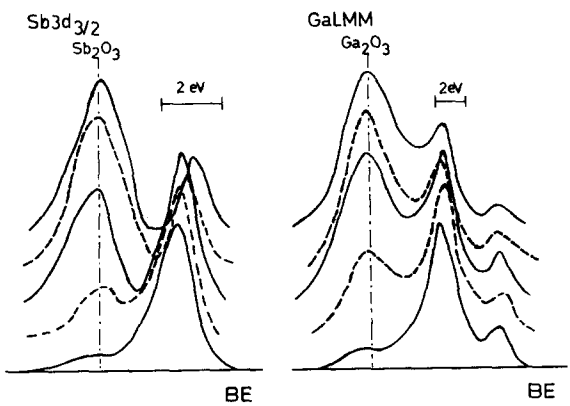

(a)

Fig. 1 *(continued)*.

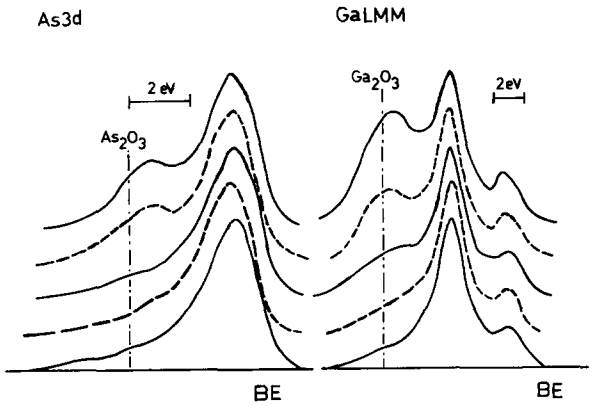

(b)

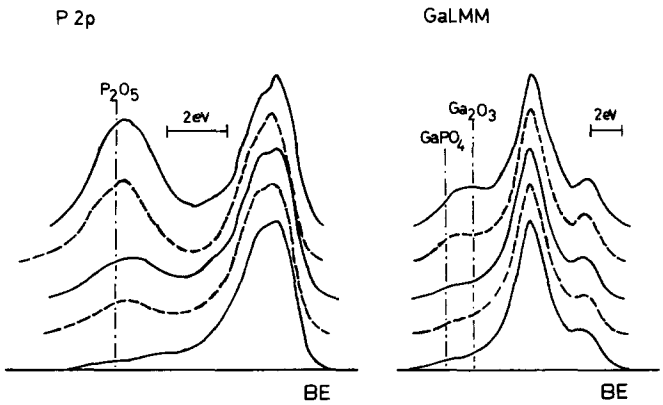

(c)

Fig. 1. Typical XPS spectra from (a) GaSb, (b) GaAs and (c) GaP as a function of air exposure time. The exposure times are several seconds, 10 min, 25 h, 554 days and 3 years from the bottom to the top in each series of spectra.

The spectra from the freshly etched surfaces of GaSb, GaAs and GaP showed slightly oxide features (about 5 Å) with approximately equal amounts of B^V oxide and gallium oxide as shown in Fig. 1. The chemical etching resulted in excess antimony and excess arsenic for GaSb and GaAs respectively and excess gallium for GaP. The amount of the excess element is estimated to be about 1 monolayer or less in this case, although the preferential etching may depend on the crystal orientation and/or the etching conditions such as pH, type of etchant and temperature[7,9].

The intensity of the shifted peak in both gallium and the B^V element, which indicates the oxide feature, increased as a function of the exposure time as shown in Fig. 1. The BE positions in typical standard oxides are indicated in the figure. Even after as long as 3 years of air exposure, all the spectra still showed clearly the unoxidized peak. The oxide thickness d(3 years) is estimated to be about 40 Å for

GaSb and 20 Å for GaAs and GaP. Figure 2(a) shows the air-grown oxide thickness of the GaB^V compounds as a function of the air exposure time on a logarithmic scale. The thickness is estimated on the basis of the relative signal intensity between the oxide and substrate after decomposition of the spectra, assuming an exponential variation of electron escape probability with depth. Figure 2(b) displays the ratio of the oxidized B^V atoms to oxidized gallium atoms (B^V:Ga(oxidized)) in the sampling depth as a function of the exposure time.

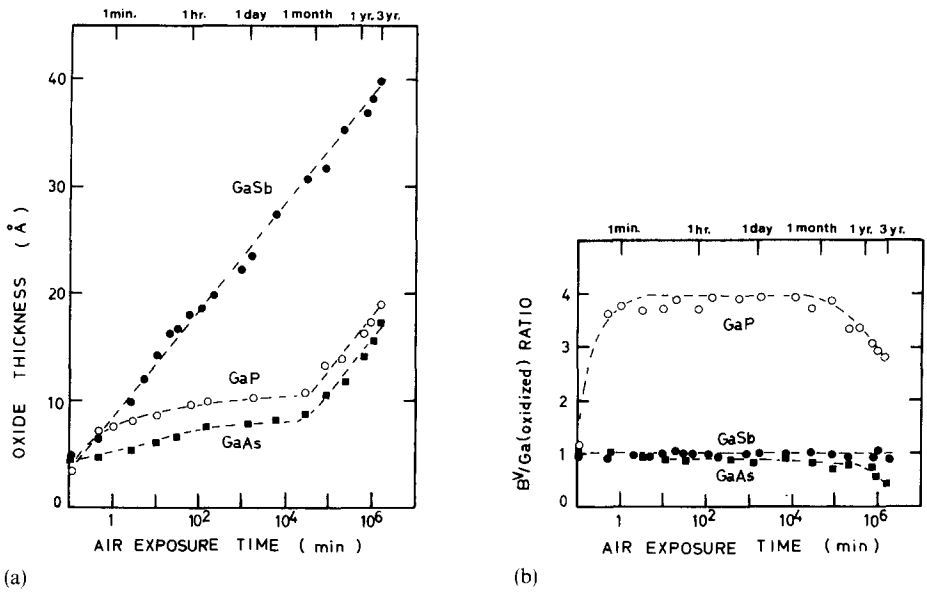

Fig. 2. (a) Oxide thickness *vs.* air exposure time for GaSb, GaAs and GaP. (b) The atomic ratio of oxidized B^V to oxidized gallium *vs.* air exposure time for GaSb, GaAs and GaP.

The oxygenated overlayer of GaB^V compound consists of gallium oxide, B^V oxide and excess gallium or excess B^V element. The overlayer compositional profiles of GaSb, GaAs and GaP are shown in Figs. 3–5 respectively. The full, broken and dotted lines represent the profiles of oxidized gallium, the oxidized B^V element, and the excess gallium or excess B^V element respectively. Measurement was performed along the direction indicated with arrows, *i.e.* the profile with increasing overlayer thickness was obtained for the surface of the growing overlayer, while the profile with decreasing thickness represents the sputter profile obtained after correction for the preferential sputtering. As can be seen, each profile shows a hysteresis curve, which implies that compositional change had occurred in the inner oxide layer during 3 years. Thus, from the shape of the hysteresis curve, we can estimate the oxide–substrate interfacial reaction.

4. DISCUSSION

4.1. Identification of the native oxide on GaB^V grown at room temperature

As shown in Fig. 1, the line shape and position of the resolved oxide peaks are

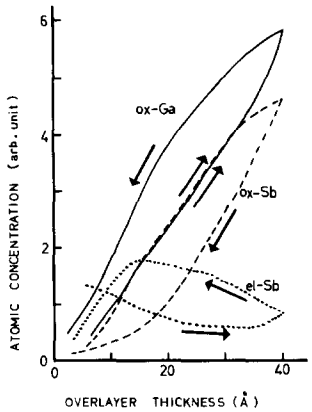

Fig. 3. Compositional profiles of the air-grown oxide of GaSb. Measurement was performed along the direction indicated with arrows. The profiles with increasing overlayer thickness are for the growing overlayer surface, while the profiles with decreasing thickness are sputter profiles for the 3-year oxide.

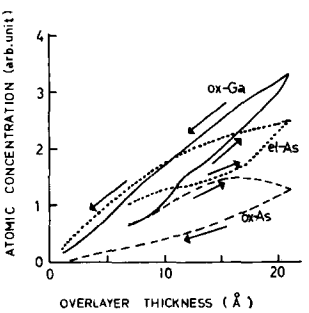

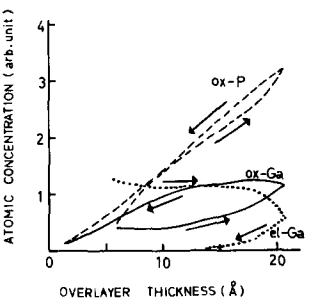

Fig. 4. Compositional profiles of the air-grown oxide of GaAs (refer to the caption of Fig. 3 for details).
Fig. 5. Compositional profiles of the air-grown oxide of GaP (refer to the caption of Fig. 3 for details).

almost constant in the corresponding series of spectra after the clear oxide peak appeared, so we will examine the spectra from the 3 year air-grown oxide (hereafter we will call it the 3-year oxide) for chemical identification purposes.

4.1.1. GaSb

Both the gallium and the antimony oxide peaks appeared immediately after the chemical etching as shown in Fig. 1(a). The ratio Sb:Ga(oxidized) remained at nearly unity throughout the oxidation process as shown in Fig. 2(b). After 3 years of oxidation, ΔE(Ga LMM − Ga 3d) of the oxide is 170.7 eV, which is in excellent agreement with that of Ga_2O_3 as shown in Table I, although the FWHM of 4 eV for the oxide Ga LMM peak was somewhat larger than that of Ga_2O_3, *i.e.* 3.3 eV. From both the value of ΔE(Sb $3d_{3/2}$ − Ga LMM) of 348.4 eV, which is again very close to $\Delta E(Sb_2O_3 - Ga_2O_3) = 348.3$ eV, and the FWHM of 1.9 eV for the oxide Sb $3d_{3/2}$ peak, the antimony oxide is undoubtedly a single species of Sb_2O_3. As the oxidation proceeded, the FWHM of the unoxidized Sb $3d_{3/2}$ peak decreased from 1.4 to 1.1 eV,

which indicates that the elemental antimony, produced by the preferential chemical etching, was consumed. Because of the small heat of formation of GaSb compared with those of GaAs and GaP it is easy to break the Ga—Sb bond and to form the true oxide even at room temperature, without the formation of the precursor metastable complexes which are formed on GaAs and GaP.

4.1.2. GaAs

The energy difference between the O 1s and the oxide As 3d for the 3-year oxide is 487.8 eV, which is larger than that of As_2O_3 by 0.8 eV (see Table I). This means that the amount of electron transfer from arsenic to oxygen in this oxide is smaller than for As_2O_3. The chemical shift (2.7 eV) of the As 3d peak referred to the unoxidized peak is also smaller than for the standard sample of As_2O_3 by about 0.7 eV as shown in Fig. 1(b). The 2.7 eV chemical shift of As 3d is very close to that of submonolayer oxygen chemisorption on a cleaved GaAs reported by Pianetta *et al.*[19] and that of a surface complex formed on room temperature oxidation ($d = 3$ Å) of cleaved GaAs reported by Iwasaki *et al.*[20] It should be noted that our oxidation stage is beyond the chemisorption stage as well as the monolayer surface complex formation stage. The FWHM of the oxide As 3d peak is equal to that of the standard sample of As_2O_3 (1.8 eV) which implies that the oxidized arsenic is probably a single phase. However, the chemical shift of the oxide Ga LMM peak is 3.6 eV, which is again smaller by 0.9 eV than that of the standard Ga_2O_3 and is nearly equal to that of the surface complex[20]. Furthermore, the FWHM of the oxide Ga LMM peak is about 1.6 times broader than that of Ga_2O_3, which suggests that the oxidized gallium consists of mixed oxide phases. This is further supported by the fact that the Ga 3d spectrum exhibited two shoulders at 1.3 and 1.9 eV, referred to the unoxidized peak located at 19.2 eV, which is in close agreement with the results by Grunthaner *et al.*[8] for a native oxide (30–40 Å) on GaAs. As shown in Fig. 2(b), the atomic ratio As:Ga(oxidized) at the outer oxide surface decreases with oxide thickness from 1 to about 0.5. The final value of about 0.5 for the 3-year oxide also agrees with that of Grunthaner *et al.*

The results on GaAs indicate that the room temperature air-grown oxide is not composed of a single phase of Ga_2O_3 and As_2O_3 but is probably a Ga–O–As network structure with two types of gallium site as suggested by Lucovsky[21]. This should be a metastable network complex which is a precursor to true oxide growth[10,20]. It is interesting that the metastable complex grows outward by at least about 20 Å, while the surface complex of cleaved GaAs and GaP was saturated by a monolayer[20]. The decrease in the As:Ga(oxidized) ratio at the oxide surface with increasing oxide thickness and/or with oxidation time is probably due to several factors, *e.g.* slow transport of the arsenic through the growing oxide film, evaporation of the arsenic oxide and the instability of the arsenic oxide in the presence of GaAs, which will be discussed in more detail later.

4.1.3. GaP

The behaviour of the room temperature air oxidation of GaP is very different from those of GaSb and GaAs. It also differs greatly from that of thermal oxidation of GaP at elevated temperatures[14,20,22]. Room temperature oxidation of cleaved GaP resulted in the formation of surface complex with P:Ga(oxidized) $\approx$ 1. The chemical shifts of P 2p and Ga LMM are 4.5 eV and 3.2 eV respectively, which

suggests that a $GaPO_x$ compound is formed that changes to $GaPO_4$ at higher temperatures with a larger chemical shift of both P 2p and Ga LMM[14,20,22].

In contrast, in the case of the room temperature air oxidation of etched GaP, the oxidized phosphorus component always overwhelms the oxidized gallium at the oxide surface (see Figs. 1(c) and 2(b)). The ratio P:Ga(oxidized) increased to about 4 after 1 min of air exposure and remained at this value for several months, then gradually decreasing to 2.8. The energy difference between O 1s and the oxide P 2p is 398.4 eV, which is nearly equal to that of P_2O_5 (398.7 eV) or $GaPO_4$ (398.1 eV), although the apparent chemical shift of P 2p (about 5 eV) is somewhat smaller than that of P_2O_5 or $GaPO_4$ (see Fig. 1(c) and Table I). Furthermore, the FWHM of the oxide P 2p peak was 2.2 eV, which is also in close agreement with the standard sample of oxide phosphorus compounds. Thus, the surface product of phosphorus oxide must be dominantly a single phase. Since the surface oxide contains only a small amount of oxidized gallium atoms, the oxide must be P_2O_5. The heat of formation of P_2O_5 (-323 kcal mol^{-1}) is much larger than that of Ga_2O_3 (-214 kcal mol^{-1}), so it is plausible that P_2O_5 forms preferentially at the surface of GaP. Although the reaction $P{=}O + Ga^{3+} \rightarrow P{-}O{-}Ga$ (formation of $GaPO_4$) is favoured on thermodynamic grounds[21], the activation energy required for this reaction to proceed may not be available at room temperature.

As has been suggested by Wilmsen[2], the oxidation of an AB alloy in which B has a higher oxidation rate than the other element leads to an initial oxide which has an outer layer of BO and an AO inner layer. This is probably the case for room temperature oxidation of GaP and the oxide surface exhibited a large ratio P:Ga(oxidized). The depth profile of the 3-year oxide of GaP in Fig. 5, which will be discussed in more detail in Section 4.2, supports the suggestion that the Ga:P(oxidized) ratio increases in the inner layer. Further, as is well known, P_2O_5 is extremely hygroscopic so that the oxidation behaviour of a phosphorus compound depends largely on the wet or dry oxidation[1,6,23]. This is the case for an anodic oxidation of GaP in which the P:Ga(oxidized) ratio of the anodic oxide surface varied greatly from sample to sample[14]. In a case of low temperature oxidation of InP[23] it is also found that the bonding state of phosphorus depends on the wet or dry oxidation.

The oxidized gallium peak is too small for the oxidized state of gallium to be determined accurately using the value of ΔE(Ga LMM – Ga 3d). As shown in Fig. 1(c), the chemical shift of Ga LMM is 4.6 eV, which is a little larger than that of Ga_2O_3/ch-GAP (4.0 eV). Additionally, the FWHM of the oxide Ga LMM peak is larger than that of Ga_2O_3. The energy difference between the oxide Ga LMM and the oxide P 2p is 57.8 eV, which is also larger than $\Delta E(Ga_2O_3\text{–}P_2O_5)$ (57.1 eV). These findings suggest that $GaPO_4$ also coexists together with Ga_2O_3 in the air-grown native oxide of GaP.

4.2. Room temperature oxide growth rate for GaSb, GaAs and GaP

Generally speaking, oxidation begins with the chemisorption of oxygen on the surface with several possible rate-determining steps such as physisorbed $O_2 \rightarrow O_2^- \rightarrow O^- \rightarrow O^{2-}$. The chemisorbed oxygen moves about on the surface and finds a stable site, where it forms bonds with the surface atoms and breaks the

substrate crystal bonds. After the nucleation of an oxide island, it grows outward and laterally until the surface is covered. Once a complete oxide layer is formed, the oxidation continues by the diffusion of metal outwards or the inward diffusion of oxygen through the oxide. Additionally, the oxidation of $A^{III}B^{V}$ compounds is more complex[2], since the growth of the oxide depends on the oxidation rate of the elements, the energy of formation of the oxide, the energy of formation of the compound, the diffusion rates of the elements through the oxide and substrate, the solubility of the oxides in each other, the evaporation rates of the oxides and/or the elements, the stoichiometry of the compound surface and the solid–solid interfacial reaction[12] etc. Thus, the oxidation of $A^{III}B^{V}$ compounds proceeds through several stages in which several discrete structures with different compositions may be involved. Since the oxidation behaviour of $A^{III}B^{V}$ compounds is very complex, it is not easy to interpret the data in Fig. 2(a) perfectly. Thus we will attempt a tentative interpretation as follows.

The data in Fig. 2(a) show that the surfaces of GaSb, GaAs and GaP examined immediately after chemical etching had already been oxidized to some degree, an average oxide thickness of about 5 Å being found for all three samples. The oxide thickness *vs.* $\log t$ data in Fig. 2(a) clearly show that the oxidation rate of GaSb is significantly larger than that of GaAs and GaP. Moreover, GaSb differs from GaAs and GaP in that the dependence of oxide film thickness on time is strictly logarithmic, over at least 7 orders of magnitude, while for both GaAs and GaP the similar logarithmic growth started after $t \approx 10^5$ min. The d *vs.* $\log t$ curve for GaAs and GaP is characterized by a region with negative curvature followed by a region of logarithmic growth. This behaviour agrees with the result obtained by Rosenberg[10] where the initial oxidation ($d \lesssim 15$ Å) behaviour on several $A^{III}B^{V}$ compounds (A = Ga, Al, In; B = Sb, As, P) was examined. The inflection indicates the onset of a new stage of oxidation. The negative curvature region for GaAs and GaP ($d \lesssim 10$ Å) may be a stage of oxide island formation. The rate of oxidation for GaP is a little larger than that for GaAs in this region. This finding agrees with the result for the initial oxidation of cleaved GaAs and GaP[20]. Since the crystal bond for GaSb is much weaker than for GaAs and GaP, the chemisorbed oxygen on GaSb immediately forms initial oxide which has little or no mobility, *i.e.* the oxide grows in nearly monolayer steps. Once the surface is covered with oxide completely, the oxide growth continues in a similar manner for the three compounds.

In the logarithmic growth region, the oxide film thickness increase per time decade is about 5 Å decade^{-1} for all three samples. The value is in agreement with that of GaAs reported by Lukes[5], although his air-grown oxide reached a thickness of about 40 Å, according to ellipsometry measurements, after 2 years at room temperature. The logarithmic growth means that the factor limiting oxide growth is not the breaking of the crystal bond or the diffusion but void formation and/or an interfacial barrier which prevents the injection of electrons into the oxide[2,5]. Further work is necessary before we decide which mechanism is the case for the present work.

4.3. Native oxide–GaB^{V} interfacial chemical reaction at room temperature

The chemical reactions that occur at oxide–semiconductor interfaces have been of considerable interest from both an academic and an industrial point of view. To

understand the long-term stability of $A^{III}B^{V}$ semiconductor devices, it is very important to investigate such reactions at room temperature for periods of up to many years. Equilibrium thermodynamics anticipates which is the favoured final state for the interface composition, while the kinetic factors determine whether this state will be reached during a given set of growth conditions. Using both Raman scattering and the ternary phase diagram, Schwartz *et al.*[12] and Thurmond *et al.*[24] showed that the relevant reactions on GaSb and GaAs yield interfacial deposits of antimony and arsenic according to the following equations:

$$Sb_2O_3 + 2GaSb \rightarrow Ga_2O_3 + 4Sb \tag{1}$$

$$As_2O_3 + 2GaAs \rightarrow Ga_2O_3 + 4As \tag{2}$$

In contrast, such an elemental phosphorus deposit was not observed for an annealed anodic oxide–GaP interface[12]. They suggested that oxide–oxide reactions occur in the film instead. Depending on the Ga_2O_3:P_2O_5 ratio in the film, the following reactions were suggested:

$$P_2O_5 + Ga_2O_3 \rightarrow 2GaPO_4 \tag{3}$$

$$3P_2O_5 + Ga_2O_3 \rightarrow 2Ga(PO_3)_3 \tag{4}$$

It is very interesting to see whether such interfacial solid–solid reactions can occur even at room temperature although an extended time period is necessary. Such information may be obtained directly by a comparison of interfacial compositions between the as-oxidized film and the same film kept at room temperature for a long time. Figures 3–5 provide some indication that such a reaction occurs even at room temperature. Each profile was measured along the direction shown by the arrows; that is, the overlayer was grown for 3 years and then it was reduced by sputtering. Since the growth rate is very slow, about 5 Å decade^{-1}, the overlayer thickness d increased by only several ångströms during the last 2 years (see Fig. 2(a)). Thus, about 3 years had elapsed between two points with equal d values of a hysteresis curve except when d is very close to the reflecting point (right-hand edge).

From Figs. 3 and 4, three features can be readily related to the change in the inner oxide composition of GaSb and GaAs: (1) increase in the gallium oxide; (2) decrease in the antimony (arsenic) oxide; (3) increase in the elemental antimony (arsenic). It appears that the results suggest that the interfacial reactions between the substrate and B^{V} oxide proceed for GaSb and GaAs even at room temperature for a prolonged time. In contrast, for GaP the amount of phosphorus oxide scarcely changed while that of gallium oxide increased for the 3 year time interval as shown in Fig. 5. Furthermore, the excess gallium atoms had been consumed for that time interval.

In order to examine more closely the data in Figs. 3–5, the poor depth resolution due to the extended escape depth must be improved. The overlayer is assumed to be composed of an n-layer system with equal layer thickness t. The normalized relative atomic density $D_{i,n}$ of the ith element in the nth layer can be

described by the following simple equation:

$$I_{i,n} = \sum_{j=1}^{n} D_{i,j} \exp\left\{ -\frac{t(n-j)}{\lambda_{i,j}} \right\} \tag{5}$$

where $I_{i,n}$ represents the normalized XPS oxide intensity of the ith element in the presence of an n-layer oxide. The variation in the X-ray flux and the instrumental constant were normalized according to a method of ref. 25. Assuming that the escape depth $\lambda_{i,j}$ is constant for each layer, we can readily calculate the relative atomic density distribution $D_{i,n}$ from the normalized $I_{i,n}$ data in Figs. 3–5:

$$D_{i,n} = I_{i,n} - I_{i,n-1} \exp(-t/\lambda) \tag{6}$$

The resulting atomic density distributions in the overlayer for GaSb, GaAs and GaP are displayed in Figs. 6–8 respectively, where the layer thickness t is chosen to be 2 Å. It should be noted that the value of $D_{i,n}$ for the growing oxide near the maximum overlayer thickness includes a large error, since the $I_{i,n-1}$ value in eqn. (6) had been changed from the measured $I_{i,n-1}$ value owing to the interfacial reaction during the long time interval, so that the profile was extrapolated in that region. Next we examine the interfacial reaction for the GaSb, GaAs and GaP systems.

4.3.1. GaSb

As can be seen in Fig. 6, the overlayer grows and produces equal amounts of oxidized gallium (Ga_2O_3) and oxidized antimony (Sb_2O_3); hence elemental antimony was scarcely detected in the growing oxide film surface. However, the depth profile of the 3-year oxide clearly shows that the amount of oxidized gallium increases, while the equal amount of oxidized antimony decreased in the inner oxide layer compared with the profiles of the growing oxide. Both the Ga_2O_3:Sb_2O_3 ratio and the amount of elemental antimony increased with a decrease in the depth for the 3-year oxide. Undoubtedly, the interfacial reaction of eqn. (1) occurs for GaSb at room temperature during the 3 year time interval, which implies that the barrier energy for the reaction should not be very high. This is further supported by the fact that the thermal oxidation of chemically etched GaSb at 100 °C for 3 min, which is also a weak oxidizing condition, resulted in a formation of an overlayer about 20 Å thick with a Ga_2O_3:Sb_2O_3 ratio of about 3. In this case additional antimony was also produced, which suggests that the reaction of eqn. (1) occurs within a very short time at this temperature. It should be noted that, in the case of room temperature oxidation, it required 2 h for the growth of the 20 Å thick overlayer, and the time was too short for the interfacial reaction to occur (see Figs. 2 and 6).

As we have already shown[11], the thermal oxidation of GaSb at higher temperatures produces a primary product of Ga_2O_3, and a large amount of elemental antimony that accumulates at the oxide–GaSb interface according to eqn. (1). In the case of anodic oxidation of GaSb, we detected a small amount of elemental antimony deposited at the interface by XPS sputter profiling[11], while Schwartz *et al.*[12] detected no elemental antimony at the as-grown oxide–GaSb interface by the Raman scattering technique. The deposition of elemental antimony in the as-anodized GaSb film cannot be ruled out since the barrier energy of the interfacial reaction (eqn. (1)) is not as high as mentioned above.

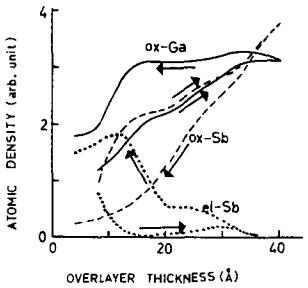

Fig. 6. Atomic density distribution of the air-grown oxide of GaSb. These profiles are obtained from the profiles of Fig. 3 after the extended escape depth correction.

4.3.2. GaAs

The major profile of the GaAs is very similar to that of the GaSb as seen in Fig. 7, although elemental arsenic is detected at the growing oxide surface because the As:Ga(oxidized) ratio decreased from 1 to 0.5 with an increase in overlayer thickness. After 3 years the amounts of both oxidized gallium and elemental arsenic increased while the amount of oxidized arsenic decreased with a decrease in the depth compared with those of the growing oxide. At the oxide–GaAs interface oxidized arsenic was scarcely detected and the interface is composed of oxidized gallium and elemental arsenic, which strongly suggests that the interfacial reaction predicted by eqn. (2) occurs. However, in this case, as mentioned in Section 4.1, the initial oxide product is not Ga_2O_3 and As_2O_3 but a metastable complex and, therefore, the interfacial reaction cannot be expressed by eqn. (2). The interfacial reaction between the metastable Ga–O–As complex and GaAs must proceed more readily than the reaction of eqn. (2) since the energy of formation of the complex is smaller than that of the stable oxide $Ga_2O_3 + As_2O_3$. The occurrence of an interfacial reaction of the type shown in eqn. (2), even at room temperature, has also been suggested by Grunthaner *et al.*[8] Their chemical depth profiles of the native oxide/GaAs grown at 25 °C showed a Ga:As(oxidized) ratio of about 2 at the outer surface, which changed to about 10 at the oxide–GaAs interface. They also detected a thin layer of elemental arsenic at the interface. Higher temperature oxidation of GaAs resulted in an increase in Ga_2O_3 and elemental arsenic and a decrease in As_2O_3 with temperature[26,27], which is fully consistent with the estimated Ga–As–O equilibrium diagram[12,24], and so the reaction of eqn. (2) is correct.

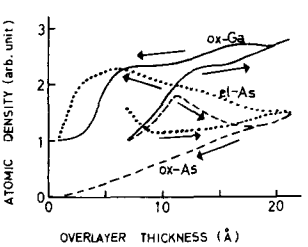

Fig. 7. Atomic density distribution of the air-grown oxide of GaAs after correction for the extended escape depth.

Schwartz *et al.*[28] estimated the growth of the interfacial elemental arsenic for anodic oxide/GaAs using Raman scattering to be as follows: $n_{As} = 10^{28} \times t \exp(-2.3 \times 10^4/T)$ atoms cm^{-2} in the region 573 K $< T <$ 639 K where t is time in seconds. If the growth rate is correct even at room temperature, it would require as much as about 7×10^{12} years for the growth of a monolayer of arsenic at the anodic oxide–GaAs interface. However, Mizokawa and coworkers[13,29] and many other groups[30–32] have reported the presence of a low concentration of elemental arsenic at the interface according to the reaction of eqn. (2). The existence of elemental arsenic at the as-anodized oxide–GaAs interface is controversial as has been reviewed by Wilmsen[1] and by Mizokawa *et al.*[29] Although no investigation on the change in the interfacial composition of anodic oxide/GaAs, kept at room temperature for a prolonged time interval, has been reported, it might show more clearly the deposition of elemental arsenic at the interface even at room temperature.

4.3.3. GaP

Figure 8 shows the changes in the overlayer composition for GaP. The profiles differ greatly from those of GaSb and GaAs. At the growing oxide surface, oxidized phosphorus (P_2O_5) always overwhelms oxidized gallium and therefore elemental gallium coexists at the oxide surface. The depth profiles of the 3-year oxide of GaP coincide with GaSb and GaAs in having an increase in oxidized gallium in the inner layer, but neither the reduction in the concentration of oxidized phosphorus nor the deposition of elemental phosphorus was observed for $d \gtrsim 10$ Å. The elemental gallium that existed at the growing oxide surface disappeared in the inner layer, which implies that the elemental gallium had been oxidized to form gallium oxide during the 3 year time interval.

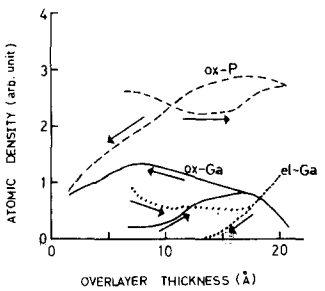

Fig. 8. Atomic density distribution of the air-grown oxide of GaP after correction for the extended escape depth.

At the interface, although the concentration of oxidized phosphorus decreases, the P:Ga(oxidized) ratio is approximately unity and no elemental phosphorous is detected. This behaviour differs greatly from that of GaSb and GaAs. Thus the following interfacial reactions analogous to those for GaSb and GaAs (eqns. (1) and (2)), did not occur for the oxide–GaP interface:

$$3P_2O_5 + 10GaP \rightarrow 5Ga_2O_3 + 16P \tag{7}$$

$$4P_2O_5 + 5GaP \rightarrow 5GaPO_4 + 8P \tag{8}$$

The changes in the Gibbs free energy ΔG for the reactions of eqn. (7) and eqn. (8) are

12.2 ± 74 kcal and -141.9 ± 182 kcal respectively[12], which means that the reactions are not always energetically favourable. As mentioned previously, the chemical etching of GaP resulted in a gallium-rich surface and the excess gallium had been consumed after 3 years as shown in Fig. 8. Thus the following thermodynamically favourable reaction probably occurs:

$$16Ga + 3P_2O_5 \rightarrow 5Ga_2O_3 + 6GaP \tag{9}$$

where the change in the Gibbs free energy is -368.6 ± 66 kcal.

Furthermore, although the reaction between the P_2O_5 and Ga_2O_3 to form $GaPO_4$ (eqn. (3)) is probably energetically favourable ($\Delta G = -59.2 \pm 70$ kcal), there was no evidence that the reaction had occurred at room temperature. At the interface the energy difference between the O 1s and oxide P 2p electrons was 398.8 eV, which is in close agreement to that of P_2O_5 (398.7 eV) and larger than that of $GaPO_4$ by 0.7 eV (see Table I). However, the apparent chemical shift of the oxide P 2p referred to the non-oxidized peak was 4.0 eV, which is smaller by 1.5 eV than the value for the P_2O_5–GaP (or $GaPO_4$–GaP) couple in Table I. We have already shown that the apparent chemical shift observed at the interface of the oxide/GaP system varied greatly with the oxidizing conditions, which is primarily attributed to the band bending of the substrate GaP[14]. Thus, the energy difference of the O 1s–P 2p data is probably more reliable than the apparent chemical shift data of P 2p for identification of the chemical state of the phosphorus oxide on GaP. Consequently, we may tentatively conclude that the room temperature oxide–GaP interface is not $GaPO_4$ but a mixture of P_2O_5 and gallium oxide. The finding that the elemental phosphorus was not deposited at the room temperature oxide–GaP interface, even after a prolonged time interval, agrees with the results for both the thermal oxidation at higher temperatures and the anodic oxidation of GaP[14,22].

4.4. Sputter artifacts and contamination

It is very important whether artifacts of sputter profiling influence the results or not. It cannot be ruled out that the ion sputtering may enhance the interfacial reactions. We have already examined the sputter effects on an oxide/GaSb system[11] using the 3 year air-grown oxide and an oxide grown in water saturated with Sb_2O_3 for 3 min, where both of the overlayer thicknesses were about 40 Å. The results showed that, despite the similar profiles of Sb_2O_3 and Ga_2O_3 from the two oxides, the amount of elemental antimony in the 3-year oxide was about 6 times larger than that of the other oxide. If sputter artifacts were present, comparable amounts of elemental antimony would be detected for both of the oxides. Thus we may conclude that the sputter-induced reactions have little effect in this work.

How hydrocarbons and/or water, which were possibly included in our 3 year air-grown oxide film, affect the results in this work is not clear at present.

5. CONCLUSIONS

The behaviour of the room temperature oxidation of GaSb, GaAs and GaP was monitored using XPS over a long time period of 3 years. The oxide–substrate

interfacial reactions were studied by depth profiling the 3-year oxide. The significant results are summarized below.

(1) The room temperature oxide on GaSb is composed of Ga_2O_3 and Sb_2O_3 in equal amounts, while for GaAs and GaP the thermodynamically stable oxide is not formed at this temperature. For GaAs, there is evidence of a formation of a metastable Ga–O–As complex, whereas P_2O_5 always overwhelms the gallium oxide at the outer oxide surface for GaP.

(2) The oxidation rate of GaSb is much larger than those of GaAs and GaP and obeys the logarithmic growth law, at least for 3 years. For GaAs and GaP, the logarithmic growth starts after the overlayer thickness reached about 10 Å. The thickness of the 3-year oxide is estimated to be about 40 Å for GaSb and about 20 Å for GaAs and GaP.

(3) The interfacial reaction between oxide and substrate occurs for GaSb and GaAs even at room temperature although an extended period of time is necessary. The resulting interface consists mainly of gallium oxide and elemental B^V.

(4) The 3-year oxide of GaP shows no elemental phosphorus at the interface. However, during 3 years, both a reduction in P_2O_5 and an increase in gallium oxide at the interface are observed. This can be interpreted by the reaction $16Ga + 3P_2O_5 \rightarrow 5Ga_2O_3 + 6GaP$, since the excess gallium, produced by a preferential chemical etching, had been consumed during the 3 year period.

(5) Poor depth resolution due to the extended escape depth is improved by simple data processing. The relation between the true atomic density $D_{i,n}$ at the nth layer and the normalized intensity data $I_{i,n}$ can be expressed by $D_{i,n} = I_{i,n} - I_{i,n-1} \exp(-t/\lambda)$ where t is the thickness of each layer.

REFERENCES

1 C. W. Wilmsen, *J. Vac. Sci. Technol.*, *19* (1981) 279.
2 C. W. Wilmsen, *Thin Solid Films*, *39* (1976) 105.
3 H. H. Wieder, *J. Vac. Sci. Technol. A*, *2* (1984) 97.
4 K. M. Geib, S. M. Goodnick, D. Y. Lin, R. G. Gann and C. W. Wilmsen, *J. Vac. Sci. Technol. B*, *2* (1984) 516.
5 F. Lukes, *Surf. Sci.*, *30* (1972) 91.
6 J. F. Wager, D. L. Ellsworth, S. M. Goodnick and C. W. Wilmsen, *J. Vac. Sci. Technol.*, *19* (1981) 513.
7 B. Schwartz, *CRC Crit. Rev. Solid State Sci.*, *5* (1975) 609.
8 P. J. Grunthaner, R. P. Vasquez and F. J. Grunthaner, *J. Vac. Sci. Technol.*, *17* (1980) 1045.
9 C. C. Chang, P. H. Citrin and B. Schwartz, *J. Vac. Sci. Technol.*, *14* (1977) 943.
10 A. J. Rosenberg, *J. Phys. Chem. Solids*, *14* (1960) 175.
11 Y. Mizokawa, O. Komoda, H. Iwasaki and S. Nakamura, *Jpn. J. Appl. Phys.*, *23* (1984) L257.
12 G. P. Schwartz, G. J. Gualtieri, J. E. Griffiths, C. D. Thurmond and B. Schwartz, *J. Electrochem. Soc.*, *127* (1980) 2488.
13 Y. Mizokawa, H. Iwasaki, R. Nishitani and S. Nakamura, *J. Electrochem. Soc.*, *126* (1979) 1370.
14 Y. Mizokawa, O. Komoda, H. Iwasaki, D. H. Shen and S. Nakamura, *J. Electron Spectrosc. Relat. Phenom.*, *31* (1983) 335.
15 M. Rubenstenin, *J. Electrochem. Soc.*, *113* (1966) 540.
16 S. P. Kowalczyk, J. R. Waldrop and R. W. Grant, *J. Vac. Sci. Technol.*, *19* (1981) 611.
17 Y. Mizokawa, H. Iwasaki, R. Nishitani and S. Nakamura, *J. Electron Spectrosc. Relat. Phenom.*, *14* (1978) 129.

18 J. H. Scofield, *J. Electron Spectrosc. Relat. Phenom.*, *8* (1976) 129.
19 P. Pianetta, I. Lindau, C. M. Garner and W. E. Spicer, *Phys. Rev. B*, *18* (1978) 2792.
20 H. Iwasaki, Y. Mizokawa, R. Nishitani and S. Nakamura, *Jpn. J. Appl. Phys.*, *17* (1978) 1952.
21 G. Lucovsky, *J. Vac. Sci. Technol.*, *19* (1981) 456.
22 R. Nishitani, H. Iwasaki, Y. Mizokawa and S. Nakamura, *Jpn. J. Appl. Phys.*, *17* (1978) 321.
23 L. L. Kazmerski, P. J. Ireland, P. Sheldon, T. L. Chu, S. S. Chu and C. L. Lin, *J. Vac. Sci. Technol.*, *17* (1980) 1061.
24 C. D. Thurmond, G. P. Schwartz, G. W. Kammlott and B. Schwartz, *J. Electrochem. Soc.*, *127* (1980) 1366.
25 H. Iwasaki and S. Nakamura, *Surf. Sci.*, *57* (1976) 779.
26 Y. Mizokawa, H. Iwasaki, R. Nishitani and S. Nakamura, *Jpn. J. Appl. Phys., Suppl.*, *17* (1) (1978) 327.
27 Y. Mizokawa, H. Iwasaki, R. Nishitani and S. Nakamura, *Proc. 7th Int. Vacuum Congr. and 3rd Int. Conf. on Solid Surfaces, Vienna, 1977*, Berger, Vienna, 1977, p. 631.
28 G. P. Schwartz, G. J. Gualtieri, J. E. Griffiths and B. Schwartz, *J. Electrochem. Soc.*, *128* (1981) 410.
29 Y. Mizokawa, O. Komoda, H. Iwasaki and S. Nakamura, *Oyo Buturi*, *51* (1982) 831 (in Japanese).
30 K. M. Geib and C. M. Wilmsen, *J. Vac. Sci. Technol.*, *17* (1980) 952.
31 P. A. Breeze, H. L. Hartnagel and M. A. Sherwood, *J. Electrochem. Soc.*, *127* (1980) 454.
32 C. C. Chang, B. Schwartz and S. P. Murarka, *J. Electrochem. Soc.*, *124* (1977) 922.